ORIGINAL RESEARCH ARTICLE   **OPEN ACCESS**

BIOSCAFFOLDS LIKE PLATFORM TO KIDNEY REGENERATION USING ANIMAL MODELS AND DIFFERENT TIME POINTS

*[*][1]Edgar Ferreira da Cruz, [1]Edson de Andrade Pessoa, [1]Andrei Furlan, [2]Giovani Bravin Peres, [2]Yara M. Michelacci, [1]Maria Aparecida da Glória, [1]Joelma Santina Christo, [1]Rafael da Silva Luiz, [1]Clara Versolato Razvickas and [1]Nestor Schor

[1]Department of Medicine, Division of Nephrology, Federal University of São Paulo, São Paulo, Brazil
[2]Department of Biochemistry, Division of Molecular Biology, Federal University of São Paulo, São Paulo, Brazil

ARTICLE INFO

ABSTRACT

Chronic kidney disease is a pandemic health worldwide. The number of people affected by this disease grows exponentially. Studies show the bioengineered organs associated to stem cells as a possibility of new strategies of development to treatments of chronic kidney disease. In this work, we developed a platform of understand steps of regeneration kidney tissues, using extracellular matrix scaffold from different species with mesenchymal stem cell from bone marrow and umbilical cord human stem cells. Our results showed the decellularization process, the repopulation of the ECM scaffold in different time points of tissue culture some biological steps of this "re" construction.

INTRODUCTION

Chronic kidney disease (CKD) is a severe problem of public health around the world. It develops in silent, progressive and irreversible form evolving to a fibrosis process and loss of metabolic and endocrine properties of the kidneys (Webster *et al*., 2017; Taal, 2016). The most challenge in management of the CKD is impaired your progress or to adopt a replacement therapy to recover functions. However, the current therapies have beneficial effects but do not be effective mostly about the comorbidities CKD related (Li *et al*., 2017; Quack and Westenfeld, 2016). Recently, several works are made using stem cells and decellularized scaffolds from lungs, hearts, livers and kidneys with enthusiastic results (Huang *et al*., 2017; Kuevda *et al*., 2017; Taylor *et al*., 2017; Hussanein *et al*., 2017; Ott, 2015). To produce a bioscaffold, several steps are required including the decellularization process. It can be performed by detergents or enzymes washes coupled to the principal artery of the organ until complete decellularization.

Corresponding author: Edgar Ferreira da Cruz
Department of Medicine, Division of Nephrology, Federal University of São Paulo, São Paulo, Brazil

Some protocols have been described the decellularization process, but none of them has been shown to be more effective than other. This process remove cellular and nuclear components, which can determine an immunological response (minimizing negative effects on the composition), biological activity of the remaining extracellular matrix (ECM) and preserve your three-dimensional architecture including a wide microvascular system (Chani *et al*., 2017; Xu *et al*., 2017; Napierala *et al*., 2017; Liu *et al*., 2017; Roth *et al*., 2017; Pu *et al*., 2017; Butter *et al*., 2016). The ECM has important role in the development of the organ scaffold-based having properties of communication, adhesion and driving the differentiation of the new tissue by mechanisms not clearly yet. These are the reason whim has called attention of researchers (Wont *et al*., 2016; Qiao *et al*., 2016; Seyler *et al*., 2017; Poornejad *et al*., 2016; Aguiari *et al*., 2017; Momtahan *et al*., 2016; Santoro *et al*., 2016). After the bioscaffold construction, repopulation step is required to viable tissue development. Mesenchymal stem cells (MSC) from different sources such as umbilical cord, adipose tissue, dental pulp and bone marrow are using in several protocols, but the development of cross species of ECM bioscaffolds and which kind of stem cell is really effective in regeneration kidney model remains unclear (Sambi

et al., 2017; Pietsch et al., 2017; Przekora and Ginalska, 2017; Huynh et al., 2017; Zhang et al., 2016; Liu et al., 2016; O'Neill et al., 2013; D'Alimonte et al., 2017; Oryan et al., 2017; Ma et al., 2017). Based on this, the purpose of this study is to develop tissue regeneration in a model of ECM kidney bioscaffold from mice, rats and pigs repopulated with rat bone marrow mesenchymal stem cell MSC-BM.

METHODS

Experimental Model: Animals used in this work, Wistar rats (Rattus norvegicus) weighing 350-500 g, mice (C57Bl6) weighing 25-30 g, from Centro de Desenvolvimento de Modelos Experimentais para Medicina e Biologia — CEDEME / UNIFESP. The pig kidneys were from donation of departamento de cirurgia experimental / UNIFESP. All protocols were submitted and approved by the Ethics Committee of this institution by the number (CEUA N° 8287270114). To the surgical proceedings the animals were anesthetized with Ketamine 75 mg/Kg and Xylazine 10 mg/Kg by intraperitoneal injection in the rats and mice. Trichotomy and skin antisepsis was performed in abdominal site with chlorhexidine-alcohol and sterile cotton gauzes. Animals were placed in surgical table at 37 °C in dorsal decubitus total nephrectomy. The incision was longitudinal, from skin to peritoneum to exposition and catheterization of aorta artery to remove the blood. Kidneys were removed preserving renal arteries, vessels and ureters, freezing in PBS -80° C for a period from 4 to 12 weeks. After, the kidneys were thawed, and the visceral fat removed gently to the decellularization process.

Building the decellularization system: To perform decellularization process were necessary the building a chamber to minimize the contamination of the ECM scaffolds that after will be repopulated in culture conditions with MSC-BM. For that, it was used acrylic of 10 mm of thickness to mount a square box with lid. Over the lid it was put three connections luer-lock (luer-to-tubing connector; Sigma-Aldrich, USA cat. N° Z261483). The first connection was to SDS (sodium dodecyl sulfate) solution, the second connection was free to other infusions and the third connection was used to use a filter 0,22 µm to avoid the pressure formation. On the opposite site of the lid, on the luer-lock output to follows the system of infusion, was connected a number 8 silicon sterile urethral catheter and it was sutured with nylon 3.0 (Ethicon, USA) in renal artery. In the left and right sides of the box, close to base, was insert a quick disconnect (Stat-o-lock quick disconnect, Sigma-Aldrich, EUA ref. n° Z4220085). Through these connections a waste system was made.

Decellularization process: The decellularization process was performed with infusion pressure of 100 mmHg by infusion pump JSB 1200 (Jian Yuan Medical Technology, Hu Nan, CN). Kidneys was perfused with distilled water and SDS 0,66% 30 minutes intermittently until the complete decellularization. Then the organs were perfused with penicillin/streptomycin 200 UI/mL / 200 µg/mL respectively per one hour. After this step, the renal cortex was removed, freezing at -80° C to other analyses that includes nucleic acid dosage, western blot, histological analysis, glycosaminoglycan electrophoresis, transmission electron microscopy, scanning electron microscopy and biochemical analysis.

Residual nucleic acid dosage of the ECM-Scaffold: To perform the nucleic acid dosage, was used 100 mg of decellularized matrix or control tissue from each species, triturated in 1 mL of Trizol (Trizol, Life Technologies, EUA ref n° 15596018) using a Polytron Pt 1200 Cl homogenizer (Kinematica AG, Littau, Switzerland). One mL (1 mL) of homogenate was transferred to propylene tubes and added 250 µL of chloroform. After, tubes were sealed, homogenized and centrifuged 12000 rpm, 15 minutes at4°C. The supernatant was discarded and added 300 µL of ethanol, gently homogenized in vortex and incubated at room temperature 2-3 minutes. Newly centrifuged 12000 rpm, 5 minutes at room temperature. DNA pellet was washed two folds with citrate buffer 0,1 M and resuspended in ethanol 75% 1 mL, incubated 15 minutes with periodic homogenization. Centrifuged 12000 rpm, 5 minutes at room temperature and the supernatant was gently removed, dried for 5 minutes in vacuum and 100 µL of DNase free water add. The dosage was performed with Quant-iT Picogreen dsDNA assay kit (Thermo Fisher Scientific, Walthan, MA, USA ref. n° P11496) according to manufacturer's instructions. To perform this assay, we used three samples of each species in duplicate.

Histological analysis: All the tissues from control kidney and decellularized ECM scaffolds were excised, fixed in 4% formaldehyde and embedded in paraffin. Tissue sections (5 µm) were obtained and used for histological analysis. H&E staining was performed according to the standard H&E protocol to evaluate the tissue morphology mostly the absence of residual cellular nuclei of ECM scaffolds. The basal membrane of each condition was evaluated by Periodic Acid-Schiff. Masson's trichrome staining from each condition was used to evaluate the collagen fibers. Alcian blue staining was used to evaluate the presence of sulfated glycosaminoglycans. All stains were purchased from Sigma-Aldrich, Saint Louis, MO, USA and the images were acquired with an Olympus BX61 microscope.

Glycosaminoglycans electrophoresis: To evaluate the glycosaminoglycans of renal and decellularized ECM scaffolds of pigs, the tissues were weighing, macerated in liquid nitrogen, dehydrated in vacuum. Dehydrated material was weighing and submitted to proteolysis in a 4 mg/mL Maxatase solution (Biocon Laboratories, Belo Horizonte, Minas Gerais, Br) in 0,05 M de Tris-HCl buffer pH 8.0, containing 1,0 M NaCl (10 mL/g of dry material). After incubation overnight at 50° C, the samples were freezing in ice bath, added trichloroacetic acid to a concentration of 10%. After 15 minutes of incubation in ice bath, the precipitate formed were removed by centrifugation (10 000 x G, 10 minutes), the pH of supernatant was adjusted to 7.0, and thus was added two volumes of ethanol. The precipitate formed after 24h at -20° C were collected by centrifugation (3 000 G for 15 minutes) and dehydrated at room temperature. The dry materials were resuspended in water and the glycosaminoglycans were identified by electrophoresis in agarose gel in 0.05 M 1-3-diaminopropane-acetate buffer, pH 9.0. After the Toluidine blue stain, the glycosaminoglycans were quantified by densitometry of the gel using the Quick Scan densitometer (Helena laboratories, USA). Graphics analysis were performed using Excel for Windows (Microsoft, USA). This assay was performed with five distinct samples of tissue control and ECM scaffolds.

Transmission electron microscopy: To analyze the ultrastructure of decellularized ECM scaffolds of kidney pigs, the samples were sectioned of cortex, fixed and analyzed at

Centro de Microscopia Eletrônica da Universidade Federal de São Paulo (CEME-UNIFESP). Samples were fixed in formaldehyde 2% + glutaraldehyde 2,5% solution, buffered in sodium cacodylate buffer 0,1M, pH 7,2 at room temperature 30 minutes, after, stored in the refrigerator with a new fixative solution until the process. To make it, samples were washed with sodium cacodylate buffer 0,1 M pH 7,2, postfixed in osmium tetroxide 2%, gradually dehydrated in ethanol 70%, 90% and 100%, with a posterior bath in propylene oxide and perform the infiltration with a mix of propylene/EPON resin in increasing concentration. Samples were embedded in pure EPON resin at 60° C for 48 h. After the polymerization, blocks were trimmed to obtain semi thin sections to delimitate the area to ultrastructural analyze. Then, the ultrathin sections were placed in fenestrated metal grids to contrast with uranyl acetate and lead citrate. The ultrastructure analyze was performed on Transmission Electronic Microscope 1200 EX II (JEOL, Japan) coupled to a GATAN Orius (USA) image capture system. Brightness, contrast and resolution adjustments were performed with Photoshop CS application.

Scanning electron microscopy: Similarly, samples of cortex from rats, mice and pigs were sectioned, fixed and sent to CEME-UNIFESP to analyze the surface of ECM scaffolds and repopulated ECM scaffolds. Samples were fixed in glutaraldehyde solution 2,5% buffered in sodium cacodylate solution 0.1 M; pH 7.2. After the fixation process, samples were washed in sodium cacodylate buffer 0.1 M; pH 7.2 and performed metallic impregnation. To make this, samples were incubated in osmium tetroxide 2% in sodium cacodylate buffer 0.1 M, pH 7.2 for 2 h, washed with sodium cacodylate buffer 0.1 M, pH 7.2 three times of 15 minutes. Incubated in tannic acid water solution 1% for 45 minutes, washed two times in distilled water (10 minutes each). After the metallic impregnation, samples were dehydrated gradually in ethanol 50%, 70%, 90% (two times of 30 minutes each) and 100% (three times of 30 minutes each) and then, samples were submitted to a drying process in a critical point chamber (Balzers CPD 030, Lichtenstein) using carbon dioxide. Following, samples were coated of a thin layer of 20-30 nm thickness of gold in equipment for this purpose (sputtering, LEICA EM SCD 500, Germany). The image acquisitions were performed in a Quanta FEG 250 (FEI, Austria) electron microscope.

Isolation and culture of mesenchymal bone marrow stem cells (MSC-BM): To isolate the marrow, the animals (Wistar rats 6-8 weeks old) were killed by cervical dislocation. Then, cells of bone marrow from both tibia and femur was obtained by flushing of marrow cavity with 1 mL of Dulbecco's Modified Eagle Medium (DMEM, Gibco, USA) complete media and collected in a 10 mL tube on ice. Cells (MSC-BM) was cultured by separation of mononuclear cells isolated from bone marrow by centrifugation in separation gradient. The centrifugation used was 1500 rpm for 30 minutes at room temperature in presence of Histopaque 1083 (Sigma-Aldrich, USA). Isolated cells were resuspended in DMEM complete medium + penicillin/streptomycin/amphotericin B solution (Gibco, USA) and placed in 25 cm2 culture flasks (TPP, USA) and maintained in incubator with 5% CO2, 37°C for 72 hours. After this period, cells in suspension was washing and discarded with 1x Phosphate buffered saline (PBS, Sigma-Aldrich, USA) and the remaining cells replacing fresh complete medium. This process was repeated every five days until achieve 80% of confluence.

Flow cytometry: Cells of second or third passages were characterized by flow cytometry using the following antibodies, all phycoerythrin (PE) or FITC conjugated and purchased from BD Biosciences, USA, were used: anti-CD90, -CD73, -Stro-1, -CD34, -CD45 and –CD11B. To make this, 106 cells were distributed to each tube and incubated for 30 minutes with 5 μL of each antibody. After the incubation, it was washed three times with washing buffer (PBS 1X; 2% FBS; 0,02% sodium azide) by centrifugation 1500 rpm for 5 minutes at 4 °C. The immunofenotyping was acquired with FACS Canto analyzer and FACS Diva software to analyze the results.

Differentiation of MSC-BM: To demonstrate the plasticity of MSC-BM, cells were stimulated to differentiation to both adipogenic and osteogenic lineages. 5X104 cells were placed in labtek chamber slide (NUNC, USA) and maintained in culture conditions with specific medium for differentiation to each lineage. The medium was prepared like described by Zuk, 2001. The adipogenic differentiation was performed in a period of 20 days. MSC-BM were maintained in medium of differentiation containing DMEM + FBS 10%; 0,5 nM Isobutyl Metylxantina (IBMX), 1 mM dexamethasone, 10 mM insulin, 200 mM indomethacin and 1% penicillin/ streptomycin, in incubator with 5% CO2, 37 °C in humidified atmosphere. Cultures were monitored daily and the culture medium changed every 3 days. The osteogenic differentiation follows same steps, however, the differentiation medium containing: DMEM + 10% FBS; 0,1 mM dexamethasone, 50 mM ascorbic acid, 10 mM β-gliicerophosphate and 1% and 1% penicillin / streptomycin, in incubator with 5% CO2, 37 °C in humidified atmosphere. Cultures were monitored daily and the culture medium changed every 3 days like described above.

Repopulation of ECM scaffolds with MSC-BM: Repopulation of ECM scaffold of pig kidney was performed with sections of cortex, sterilized with peracetic acid (PAA, Sigama-Aldrich, USA) 1:1000 in 20% ethanol, placed on the bottom of the 24 wells culture plate and applied 106 MSC-BM at the surface of ECM scaffolds, added complete medium, and this, changed every 5 days until the time points 5 days, 10 days, 20 days and 90 days. After this process, the samples of ECM scaffolds were analyzed or stored at -80 °C to futures analyzes as well as the culture scaffold supernatant at each time point.

FTIR-spectroscopy: To understand part of the cellular behavior, we performed analyze of culture supernatant using control medium, and the culture supernatant of each time point 5 days, 10 days, 20 days and 90 days to observe if there some compatible alterations with cellular metabolism. To performing this, samples of 5 μL of each time point was applied in triplicate to a gold coated slide, drying at room temperature and analyzed with the Nicolet iN 10 FTIR spectroscope (Thermo Fisher, EUA) in transmission mode with liquid nitrogen cooled detector and the graphs represent the average of 64 acquisitions per sample.

Western blot: To analyze the presence of lineage differentiation markers from MSC-BM to renal cells, we performed the western blot analysis of the repopulated ECM scaffolds homogenate from each time point of culture and the homogenate from tissue control for podocin, K / Cl (KCC2 protein) channels and aquaporin 2 markers. The protein samples were extracted by standard protocol prepared in laemli buffer and applied 30 μL for well in a 10% acrylamide gel,

running at 100 v, transferred for 1 h in a Polyvinylidene Fluoride (PVDF) membrane (Bio-Rad, USA). The molecular weight used was the Amersham ECL Rainbow Molecular Weight (GE, USA, ref n° RPN800E). All antibodies were purchased from Abcam, UK.

Biochemical determination: To continue analyzes of the culture supernatants, samples of each condition of the culture supernatant, was analyzed in triplicate for glycose, lactate dehydrogenase (LDH), creatine phosphokinase (CPK). Both alkaline phosphatase (ALP), gamma glutamyl transpeptidase (GGT) were measured from the homogenate of repopulated ECM scaffolds at each condition. The biochemical analyses were performed with a Dimension RXL Max (Siemens, AG).

Human stem cells assay: To study the cross-species interactions between animal ECM scaffolds and human stem cells we performed the incubation with ECM scaffold from kidney Wistar rat with human umbilical cord stem cells (kindly provided by Dr Sibov and Dr Pavon). These cells (106 over the scaffold), after 24 h of incubation over the ECM rat kidney scaffold, received 40 μL of Molday ION Rhodamine B nanoparticles (Molday, USA) in complete DMEM medium and were maintained in culture conditions with DMEM + 10% FBS, 37 °C in humidified atmosphere. After the incubation period, the ECM scaffold were frozen at vapor-phase nitrogen and then, prepared on slides for immunofluorescence. To perform it, was used anti-collagen IV antibody (Abcam, USA). The image acquisitions were performed with a Leica TCS Sp8 CARS (Leica, USA) confocal microscope.

Statistical analysis: The data were input in a Microsoft Excel 2000 database and the statistical analysis were performed using the Statistical Package for Social Sciences (SPSS version 23.0) (Chicago, Illinois, USA). The results were expressed by media ± SEM, used t-test, and $p < 0,05$ was considered significant.

RESULTS

The construction of the apparatus to descellularize the pig kidney was followed with tests to validate their use. The testing, we filled until the border line with each of the solutions that met the ECM scaffold at room temperature and 37°C for 20 days to check for possible leaks. It was performed three times, once without leaks, the equipment was used for decellularization of the kidney of as shown in Figure 1A. Decellularization process was interrupted by visual inspection of the ECM scaffold translucency. Moreover, it was observed differents time points to obtaining an ECM scaffold completely decellularized to each species (Figures 1B—1G). To evaluate the effectiveness of decellularization and identify the presence of DNA residues, it was performed chemiluminescent assay with Quant-it PicoGreen ds DNA kit to detect it in ECM scaffolds of all species in this study, and we found a prominent decrease of DNA quantity in the mice ECM scaffold vs control tissue ($12,5 ± 3$ vs $480 ± 200$ ng / mL; $p< 0,0001$, t-test analysis). Similarly, results were found at the analysis of the rat and pig analysis $30 ± 7$ vs $535 ± 83$ and $49 ± 38$ vs $1000 ± 52$ respectively (Figures 1H — 1J). Histological analysis of all species involved in this study, shown the natural renal morphology, presence of nuclei and collagen architecture used as control tissue by H&E, PAS and Masson's Trichrome staining respectively (2A — 2I). Besides at the ECM scaffolds was revealed by H&E staining the absence of cellular nuclei compared to images of tissue control reinforcing the effectiveness of decellularization process (Figures 2J — 2L). Periodic Acid Schiff staining shown that although the decellularization process was performed with a detergent, the basal lamina remains preserved (Figures 2M — 2O). And with the Masson's Trichrome staining we observed that the collagen architecture was not affected by this washing (Figures 2P — 2R). The immunofluorescence was performed at the conditions control and decellularized at the renal tissue
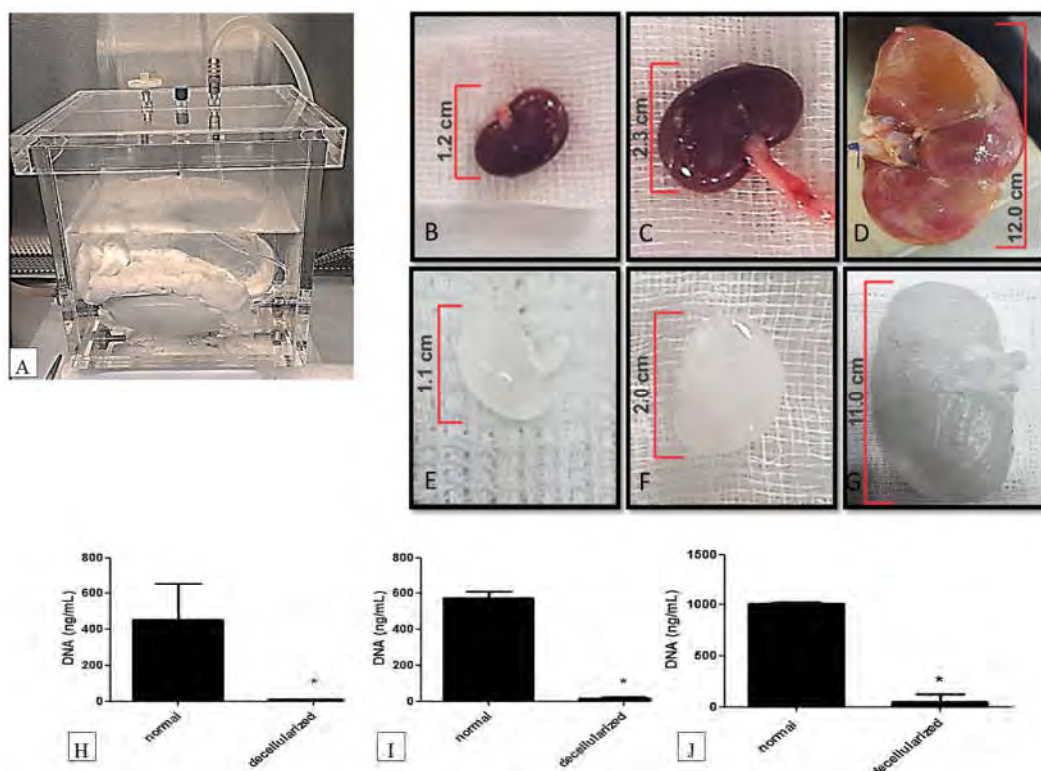

Figure 1. Decellularization process and quantification of DNA residues: A. The equipment to decellularize; B, Natural mouse kidney; C, Natural rat kidney; D, Natural pig kidney used as tissue control and E, mouse decellularized kidney; F, rat decellularized kidney; G, decellularized kidney pig. H-J quantification of DNA residues from each ECM scaffolds species. T-test analysis, p < 0.0001

and ECM scaffolds from mice, rats and pigs to identify the presence of collagen IV, fibronectin and laminin. These proteins are crucial to the repopulation process with MSC-BM. The results showed the presence of collagen IV in the three-control species (Figures 3A — 3C) as well as the presence of fibronectin (Figures 3D — 3F) and laminin (Figures 3G — 3I).

appearance of emptiness to the ECM scaffold structure. Moreover, it was possible to observe part of the architecture of the recipient to MSC-BM to perform the repopulation process (Figures5A—5F). Giving sequence to repopulate the ECM scaffolds, MSC-BM was used at the second or third passage (Figure 6A).
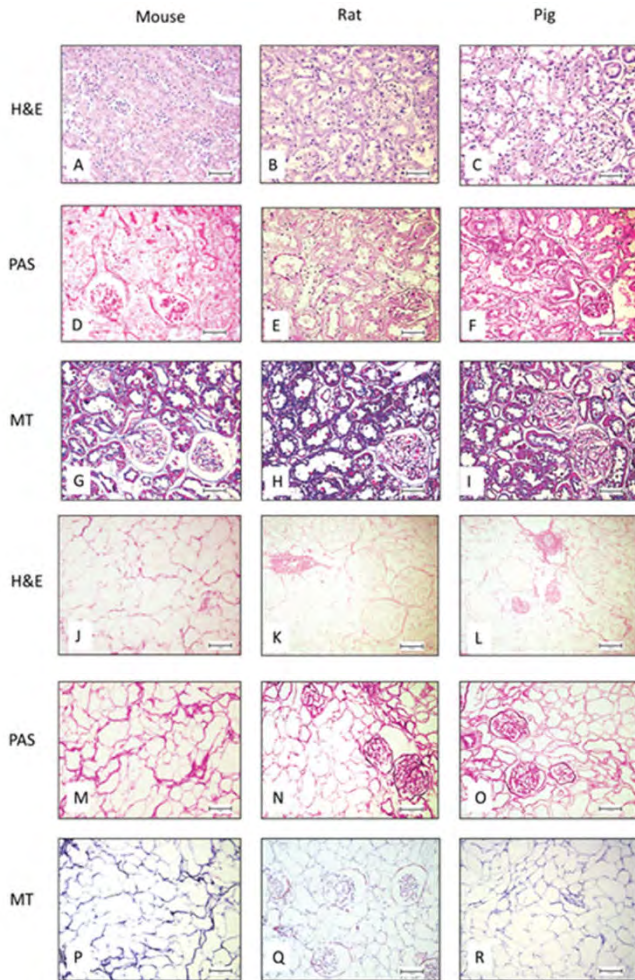

Figure 2. Histological analysis from tissue control and decellularized ECM scaffolds from mouse, rat and pig models. H&E staining from control tissue A-C; PAS staining from tissue control D-F; Masson's Trichrome staining from tissue control G-I. Similarly, to control tissues, we performed same histological analysis at the decellularized ECM scaffolds from each species. H&E staining J-L; PAS staining M-O and Masson's Trichrome P-R
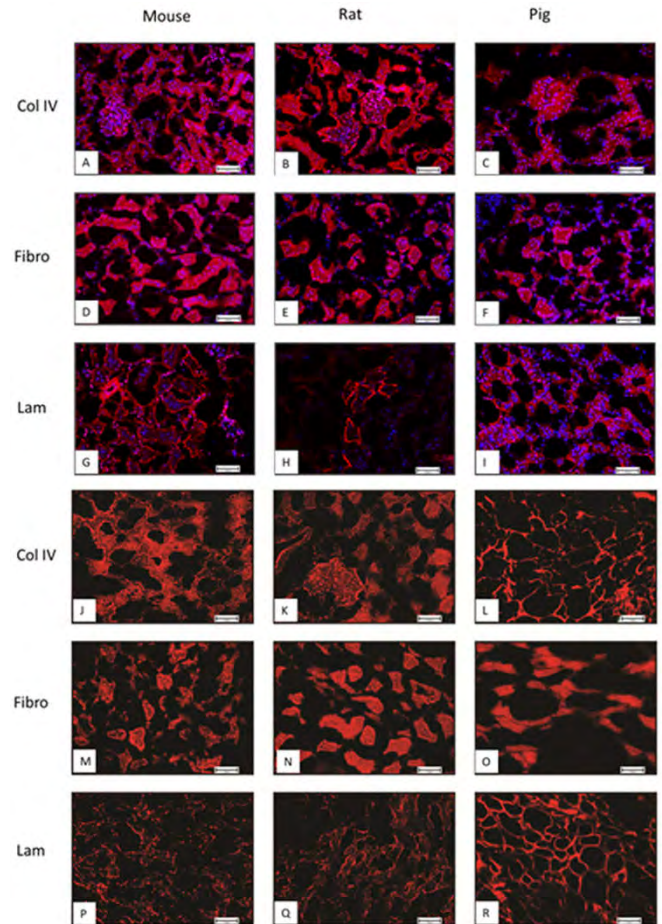

Figure 3. Immunofluorescence of control tissue and decellularized kidney scaffold from mouse, rat and pigs for detection of collagen IV, A-C; fibronectin, D-F and laminin, G-I. At the decellularized, collagen IV, J-L; fibronectin, M-O; and laminin P-R

At the ECM scaffolds this assay shown that the collagen IV, (Figures 3J — 3L) fibronectin (Figures 3M — 3O) and laminin (3P — 3R) remains also preserved after the decellularization process. Additionally, the ECM scaffolds constituents, we performed glycosaminoglycans electrophoresis only with the pig ECM scaffolds because was with this ECM scaffold that we performed the repopulations assays, and by this technique, was possible to observe an expressive decrease of total glycosaminoglycans (Figure 4C — 4D), chondroitin sulfate and heparan sulfate fractions and a partial decrease in the fractions of dermatan sulfate, (Figure 4A- 4B). Furthermore, it was possible to observe glycosaminoglycans decrease at the ECM scaffolds by Alcian Blue staining (Figures 4E—4H). Ultrastructure study of the ECM scaffolds were performed the scanning electron microscopy (SEM) and transmission electron microscopy (TEM) and it was observed cells absence in scaffolds and the decellularization process gave an

Cells cultured with DMEM + 10% FSB, 37 °C, 5% CO2 was used to perform the immunofenotyping by FACS analysis, and we observed that in this passage after the incubation, 96.4% were positives for CD90, 45.9% positive to CD73, and 47% were positives for STRO-1 phenotype. Besides, the immunomarkers CD34, CD45 and CD11b were decreased 0.1%, 0.1% and 0.1% respectively (Figure 6B). In addition, we performed the differentiation of MSC-BM for adipogenic and osteogenic lineages stained with oil red and alizarin red staining, and through and these techniques it was possible characterize the MSC-BM cells and validate the isolation protocol to repopulate the ECM scaffolds (Figure6C—6D). Thus, ECM scaffolds were repopulated with MSC-BM. These assay evaluations were performed by scanning electron microscopy and shown the ECM scaffold surface topography at the two conditions, decellularized and repopulated with MSC-BM. The images showed at the decellularized ECM scaffold surface, a fine roughness at a magnification of 1,948 X (Figure 7A) and confirmed by an image at a 10,000 X magnification (Figure 7B). Over the repopulated ECM scaffold, at the incubation time of 20 D (7C — 7D) we observed adhered cells at the ECM scaffold surface and after 90 D we can observe the tissue formation over the ECM
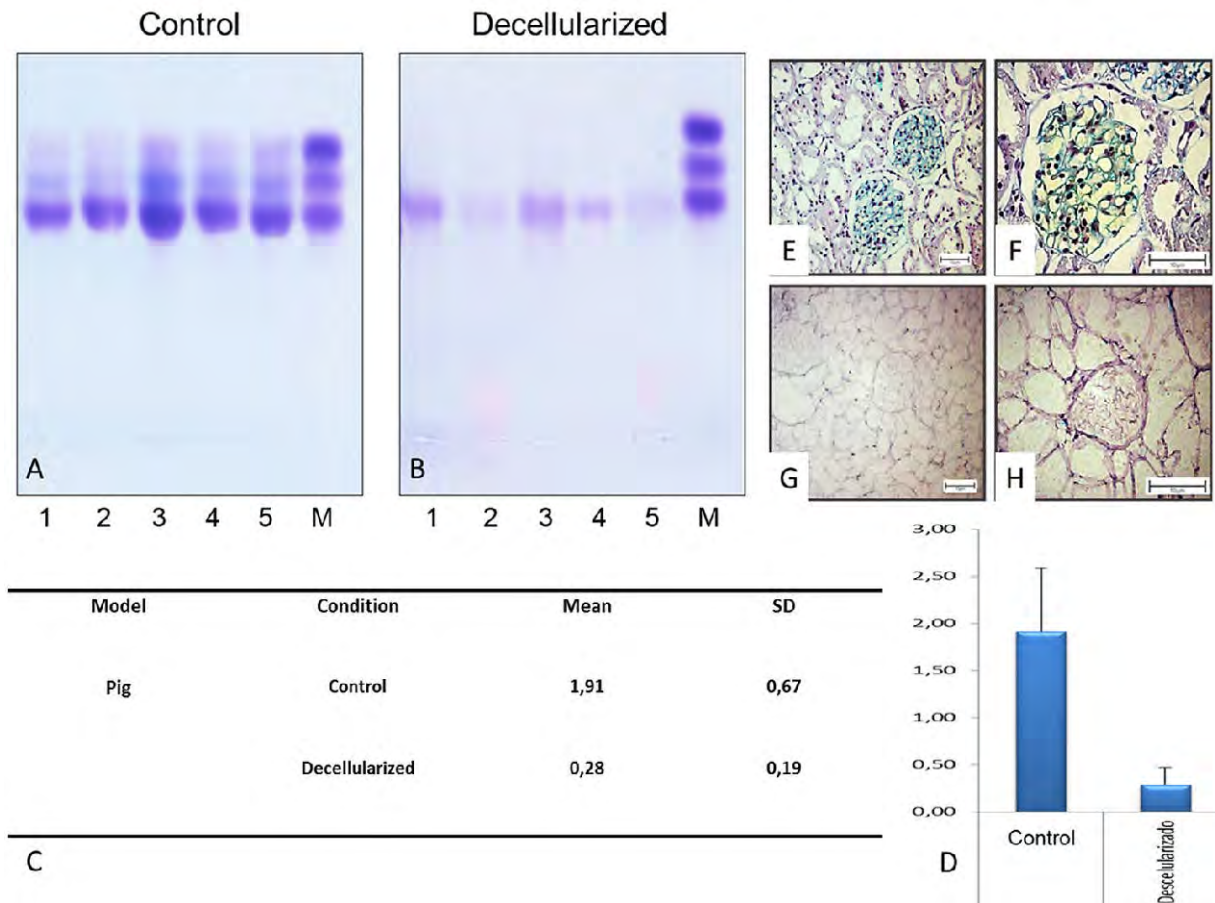
Figure 4. Glycosaminoglycans electrophoresis. A, Electrophoresis from kidney pig used as a control. It was performed with five distinct samples and marker. The marker represents from top to bottom chondroitin sulfate, heparan sulfate and dermatan sulfate. B, At the ECM scaffolds from pig, we observed a decrease of glycosaminoglycans excepting the dermatan sulfate. C-D, Quantification of glycosaminoglycans (ng / mg) of dry weight. E-F, Alcian blue staining from pig tissue control, the blue dye have affinity for glycosaminoglycans (magnification 20X and 40X). G-H, Alcian blue staining from ECM scaffolds (magnification 20X and 40X) shown decrease of glycosaminoglycans
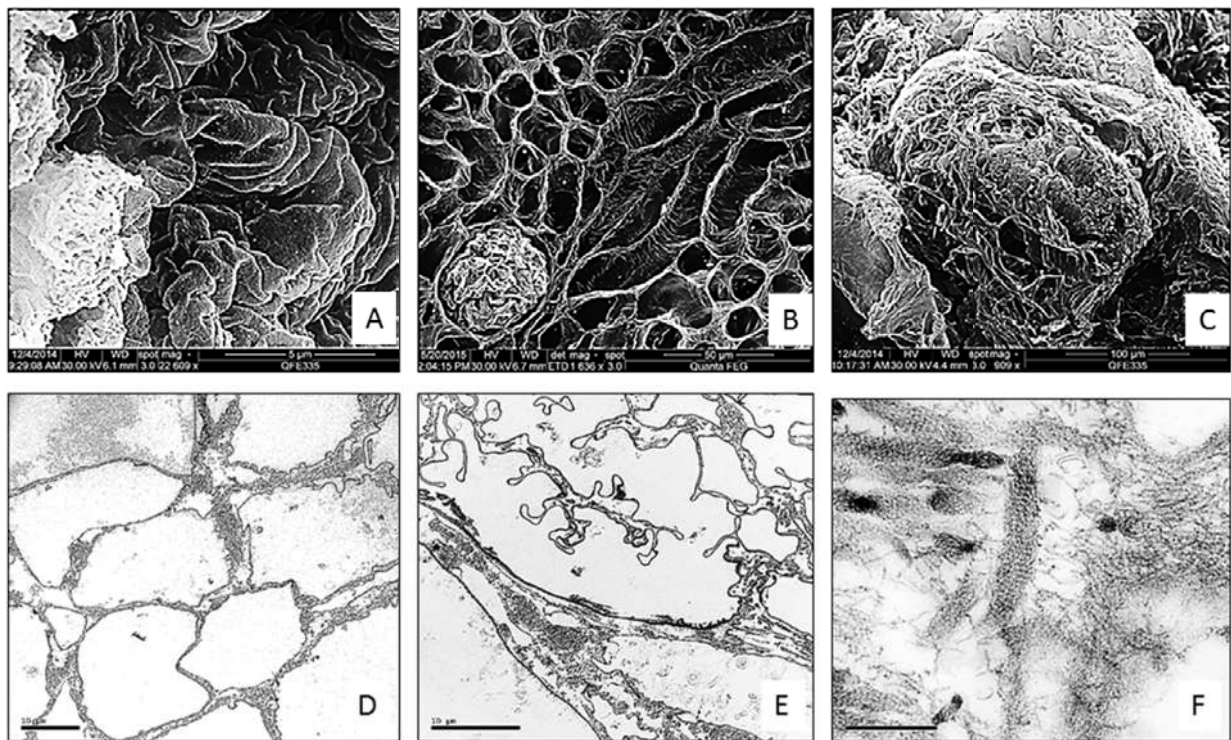

Figure 5. Electron microscopy of decellularized ECM scaffold. A, Scanning electron microscopy of decellularized ECM scaffolds from mouse; B, rat; C, pig. Transmission electron microscopy of decellularized ECM scaffolds from each species, D, mouse; E, rat; F, pig

scaffold surface reinforcing this capacity of MSC-BM (Figure 7E — 7F). To understand part of the cellular behavior of the adhered MSC-BM to the ECM scaffold in differents incubations periods, FTIR spectroscopy assay was conducted with the supernatant of the cultured ECM scaffold with MSC-BM at each time point. The graphs shown differences at each time point and these data mainly at the 5 D time, we observed a pronounced difference at the vibrational spectra showing a metabolic high rate at this time point. This data suggest that is in this in-vitro period that cell adhesion and the first stages of MSC-BM transdifferentiation occurs, inducing these metabolic changes observed by the spectral change between the control and 5 D supernatant samples (Figure 8A — 8D).

These data were confirmed by biochemical analysis of these supernatants. Biochemical analysis of the supernatant at each time point was performed to evaluate the glucose consumption and to discard the possibility of the spectral changes observed at FTIR spectroscopy analysis could have been caused by liberation of stress or death biomarkers such as creatine kinase (CK) and lactate dehydrogenase (LDH). The results shown a pronounced decrease of the glucose present at the supernatant mostly at the 5 D time point compared to the control medium, confirming the FTIR spectroscopy analysis. At the sequent time points, we observed a progressive decrease of glucose consumption and in all time points undetectable levels of CK and DHL biomarkers (Figures 8E — 8F).
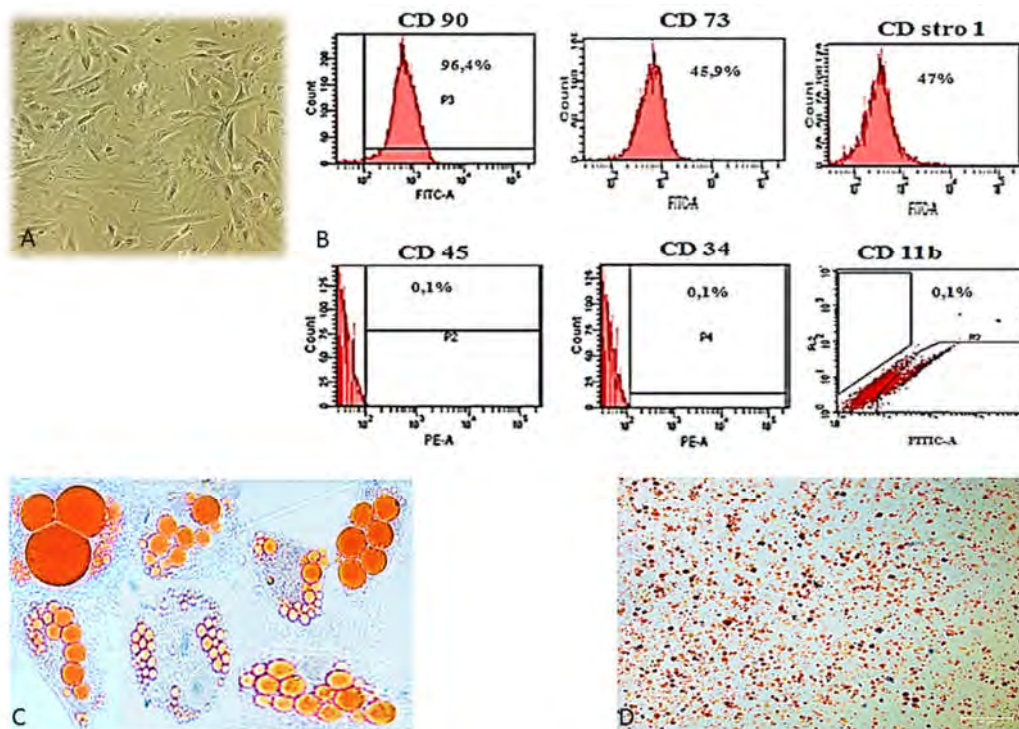

Figure 6. Culture and characterization of MSC-BM: A, cells at 2-3 passage. B, Immunophenotyping of MSC-BM by FACS analysis. C, Adipogenic differentiation; D, osteogenic differentiation
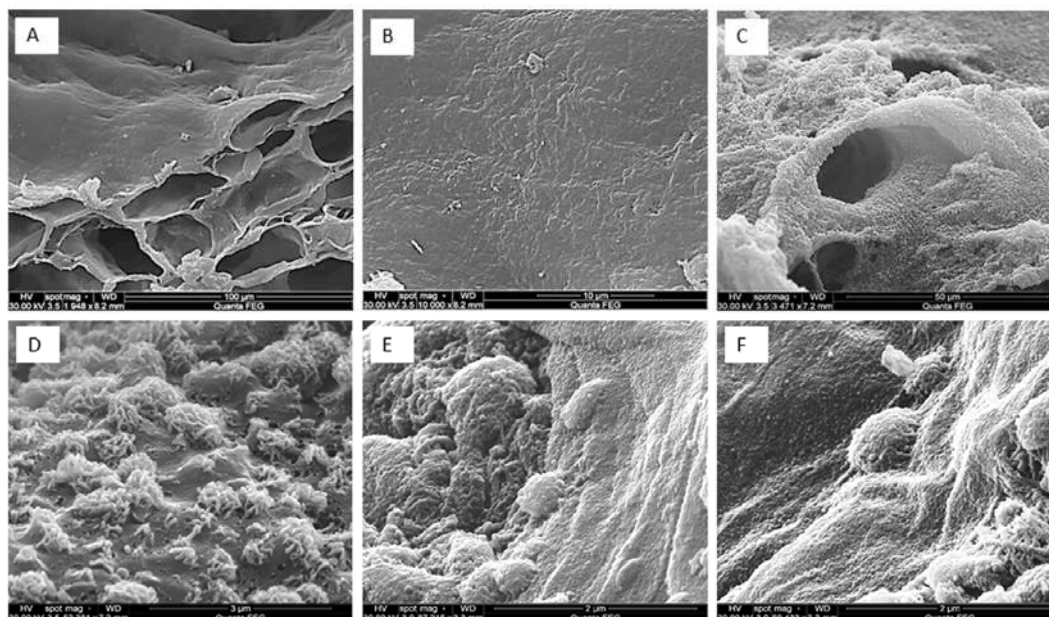

Figure 7. A, Scanning electron microscopy of pig ECM scaffold magnification of 1,948 X. B, 10,000 X shown the surface of decellularized ECM scaffold. C-D, after cultured 20 D with MSC-BM shown the cellular adherence at the scaffold surface. E-F, after cultured 90 D with MSC-BM shown the tissue formation at the scaffold surface

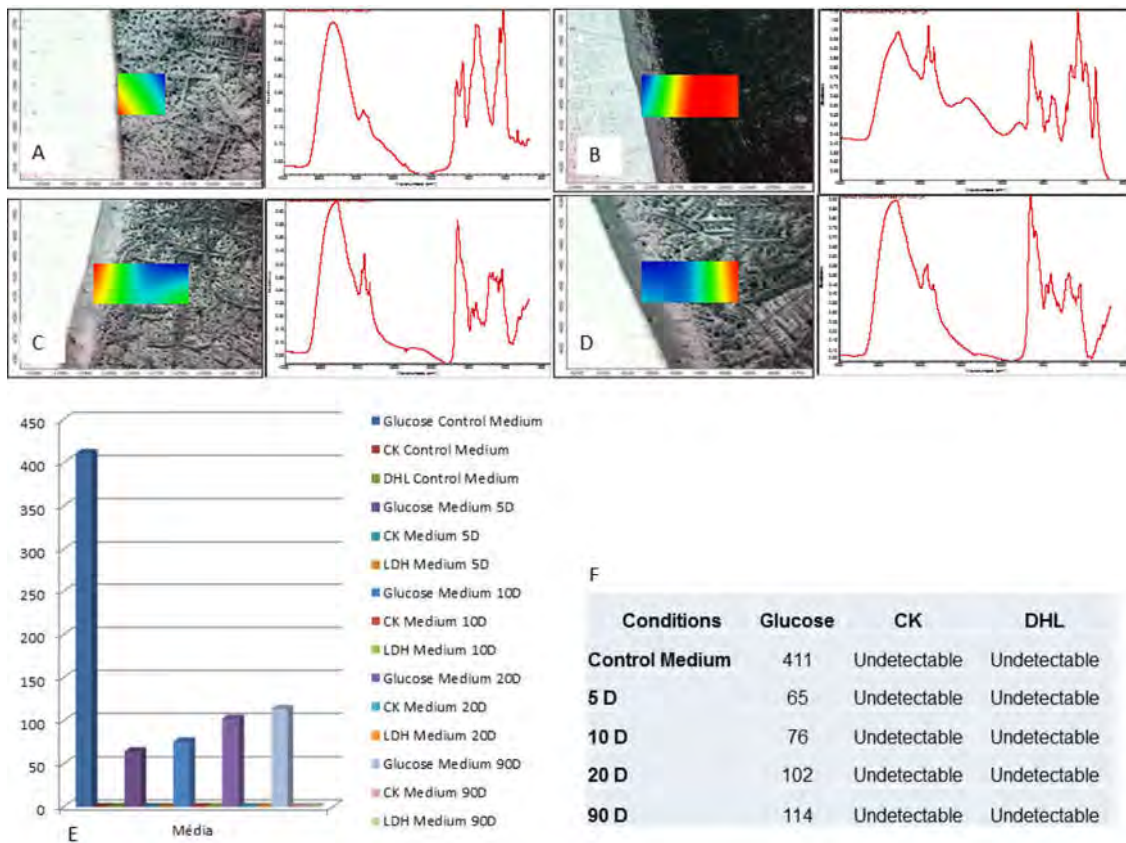| Conditions	Glucose	CK	DHL
Control Medium	411	Undetectable	Undetectable
5 D	65	Undetectable	Undetectable
10 D	76	Undetectable	Undetectable
20 D	102	Undetectable	Undetectable
90 D	114	Undetectable	Undetectable

Figure 8. FTIR spectroscopy of repopulated ECM scaffold supernatant. At the time points A, Zero that represents culture medium DMEM before culture, used as a control. B, after 5 D of culture; C, after 10 D of culture; D, 20 D of culture. E, Biochemical analysis of culture supernatants of same time points shown the glucose consumption at each time point and absence of LDH and CK enzymes. F, Table of biochemical analysis
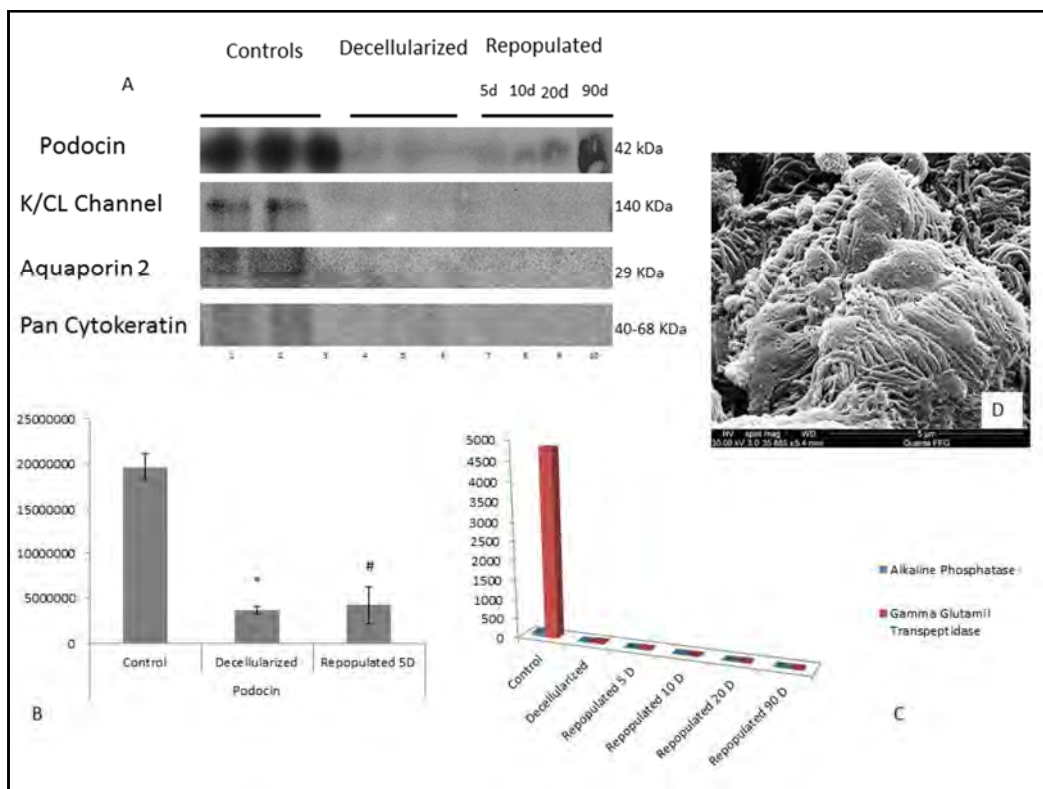

Figure 9. Western blot analysis from repopulated pig ECM scaffolds at 5 D, 10 D, 20 D, 90 D cultured and controls for podocin, K / CL (KCC2 protein) channel, aquaporin 2 and Pan cytokeratin, shown in a time-dependent manner the expression of podocin and the absence or in an undetectable form the expression of the other proteins. B, Statistical analysis for the expression of podocin * decellularized VS control p < 0.001; # repopulated VS decellularized p < 0,05. Analysis were performed with SPSS 23.0. C, Biochemical analysis from the homogenate of tissue control, decellularized and repopulated at each time point for alkaline phosphatase and gamma glutamyl transpeptidase

Repopulated ECM scaffolds cultured at 20d shown the presence of cells with morphology podocyte-like by scanning electron microscopy. To confirm these images and to evaluate other possible MSC-BM transdifferentiation, we performed western blot analysis of the ECM scaffolds homogenate from each cultured time point. Indeed, the results showed cells that express podocin, a specific protein of renal podocytes and this expression was time dependent. The ECM scaffolds repopulated and cultured until 90d showed over expression than 20d cultured repopulated ECM scaffolds.
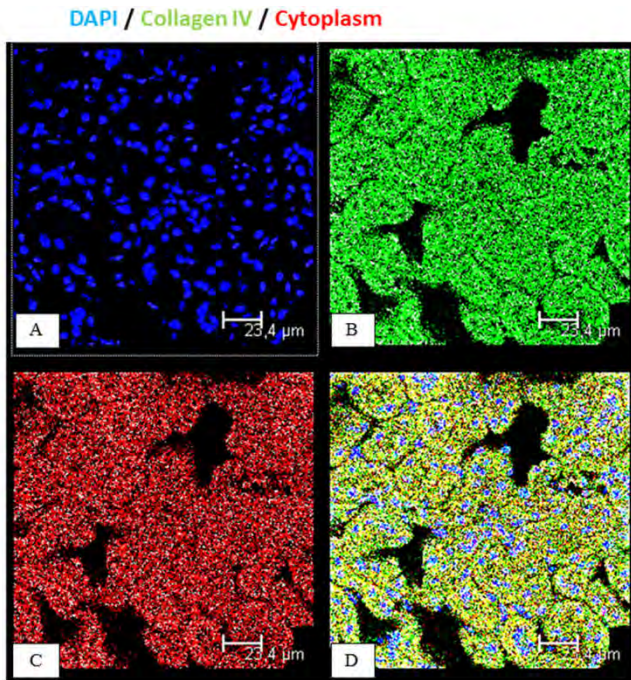

DAPI / Collagen IV / Cytoplasm

Figure 10. Confocal image of rat ECM decellularized scaffold repopulated with human umbilical cord stem cell. After 5 days in culture, we observed the cells adhered at the scaffold surface
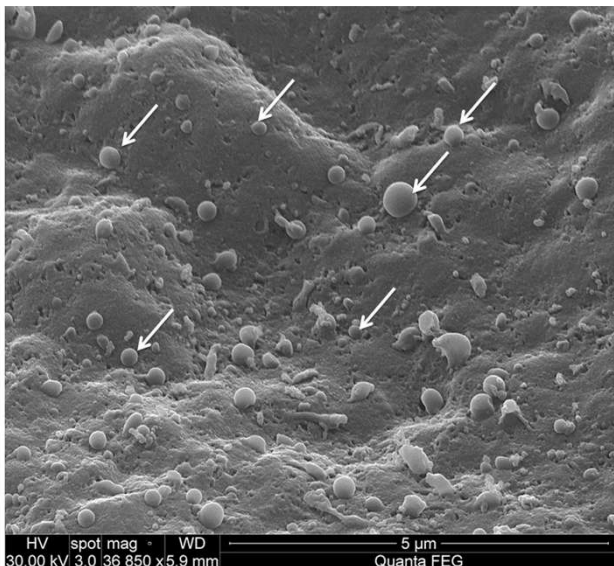

Figure 11. Pig ECM scaffold repopulated with MSC-BM after 90 days of incubation. Presence of tissue formed. White arrows show extracellular vesicles

Besides, were not possible to detect the other renal proteins evaluated, K / Cl (KCC2 protein) channel, aquaporin 2 and pan cytokeratin by western blot analysis, it is can due the undetectable quantity of these proteins or MSC-BM at the transdifferentiation in this model in-vitro do not express these

proteins. Similarly, the biochemical analysis of the homogenate to alkaline phosphatase and gamma glutamyl transpeptidase showed a gradual decrease of these enzymes. These data suggest that the enzymes current at the homogenate were present in the ECM scaffold and not from the cells that repopulated those (Figures 9A — 9D). Another assay was realized in order to verify how human stem cells cross-grafted with an animal ECM scaffold behaved and the results were promising. The confocal images showed the human umbilical cord stem cells adhered to rat ECM scaffold, suggesting new developments in this research involving xeno ECM scaffolds and human cells (Figure 10).

DISCUSSION

International statistics have showed more than 500 million people with CKD worldwide. Furthermore, 50% of this people may die at the end of three years of dialysis (Kim *et al*., 2017; Inker *et al*., 2017). The modalities of dialysis as a part of the therapy of that promote other comorbidities related to persistent inflammation caused by this treatment (Sumida *et al*., 2017; Yoong *et al*., 2017). Another replacement therapy is kidney transplantation, but, the lack of donors is a serious problem and has contributed the increase number of demands. Furthermore, maintain this population on a permanent dialysis program may affect the effective costs of health (Thuret *et al*., 2016; Bailey *et al*., 2016; Zhou *et al*., 2016). Research groups around the world have been dedicated to finding new approaches to treat CKD. Among them, bioengineered tissues ECM scaffolds-based and stem cells in an attempt to regenerate lungs, livers, kidneys, hearts and this has emerged causing expectations (Zhou *et al*., 2017; Wang *et al*., 2017; Guyette *et al*., 2016; Remuzzi *et al*., 2017). In the present work, we investigate the use of ECM scaffolds from mice, rats and pigs as a platform to understand the development process of a regenerated tissue in different models and time points of investigation.

Our results shown about the decellularization process, a 0.66% concentration of SDS as an optimal concentration option. In fact, was the lowest concentration tested able to decellularising the kidneys with minimal residues of DNA reminiscent and preserving structures as the basement membrane, collagen IV as well as adhesive proteins such fibronectin and laminin. The extracellular matrix, their molecules and receptors have a crucial role in the development and repair of tissues. It offers support to cellular organization and participates of cell growth and proliferation by the interaction with growth factors and cytokines. These interactions are describing since the kidney embryogenesis (Costa *et al*., 2017; Gonçalves *et al*., Song *et al*., 2016). Glycosaminoglycans are large sequences of polysaccharides protein-bound forming the proteoglycans. Since the kidney formation, the proteoglycans observed in the basement membrane differ from those produced by surrounding mesenchyme. The heparan sulfate named perlecan is present in ureteric bud basement membrane. Chondroitin sulfate and heparan sulfate chains belongs to syndecans which are transmembrane proteins and glypicans proteins which are proteins glysosylphosphatidiylinositol-anchored membrane respectively. These data corroborate our results, after the decellularization, the electrophoresis of glycosaminoglycans showed the loss of these glycosaminoglycans membrane-bound by the SDS washing (Mende *et al*., 2016; Holmes, 2014; Tang *et al*., 2016; Nigam and Bush, 2014; Song, 2016; Afratis *et al*., 2017; Matsuo and Kimura-Yoshida, 2014;

Peloso *et al*., 2015; Choi *et al*. 2015). The electron microscopy revealed structures in all species involved in our study with emptiness aspect reinforcing the effectiveness of the decellularization process and results similar to observed by other authors. To prepare these ECM scaffolds to the culture assay, they were sterilized before their use with a solution of peracetic acid diluted in ethanol, as described by Yoganarasimha *et al*. although they done this protocol to an artificial scaffold, it is a protocol easily adapted to ECM scaffolds. Using it, we do not observe any occurrence of contamination in our experiments (Yoganarasimha *et al*., 2014). About our ECM scaffold repopulation assays, we observed by scanning electron microscopy mainly at the times 20 days, cellular adhesion and the early cell organization and through the 90 days of incubation the tissue formation observed by widespread cellular distribution and the presence of others important factors that may influence the cellular adhesion, communication cell-cell and the transdifferentiation such as the extracellular vesicles (Figure 11). These vesicles may play a role of development together with growth factors and cytokines present in the extracellular matrix. An elegant work conducted by Huleihel L *et al*. (2016) showed the presence of extracellular vesicles in both, natural fresh scaffolds and industrially processed scaffolds (Huleihel *et al*., 2016). In fact, the kidney embryogenesis describes a complex environment that involves the formation of the extracellular matrix in a presence of growth factors, and other molecules in a dynamic structural remodeling, and this turn over process, drives an extracellular building in a layer-to-layer form allowing the inclusion of several molecules and extracellular vesicles, becoming the extracellular matrix in a very enriched structure (Grobstein, 1956; Grobstein 1956). In addition, other studies described the human kidney development can be mimicked in models of amphibians and avian, showing a biological mechanism highest conserved through the evolution and these evidences may support our hypothesis that ECM scaffolds from pigs and human mesenchymal stem cells, such as showed in figure 10, can be a key way to evolution of the regenerative challenges. However, these conjectures need to be confirmed with other studies (Sariola *et al*., 1984; Sariola *et al*., 1984).

Conclusions

In this research we conclude that the bioengineered scaffolds can be used as a platform to study to understand the kidney regeneration process. The decellularization method using the SDS detergent is effective to build a scaffold. The removal of some glycosaminoglycans of the scaffold by the washing do not interfered in cellular adhesion. Repopulating ECM scaffold is a dynamic process and have participation of growth factors, cytokines and extracellular vesicles to maintain the tissue homeostasis. Besides, the use of human umbilical cord stem cells cross-grafted with an animal model of rat ECM scaffold, did not alter the ability of cells to adhere to this substrate. However other studies should be conducted to validate these functions in a translational model.

Acknowledgements

REFERENCES

Afratis NA, Nikitovic D, Multhaupt HA, Theocharis AD, Couchman JR, *et al*. 2017. Syndecans - key regulators of cell signaling and biological functions. FEBS J. Jan; 284(1):27-41.

Aguiari P, Iop L, Favaretto F, Fidalgo CM, Naso F, *et al*. 2017. In vitro comparative assessment of decellularized bovine pericardial patches and commercial bioprosthetic heart valves. *Biomed Mater*. Feb 3;12(1):015021.

Bailey PK, Ben-Shlomo Y, Tomson CR, Owen-Smith A. 2016. Socioeconomic deprivation and barriers to live-donor kidney transplantation: a qualitative study of deceased-donor kidney transplant recipients. *BMJ Open*. Mar 2;6(3):e010605.

Butter A, Aliyev K, Hillebrandt KH, Raschzok N, Kluge M, *et al*. 2016. Evolution of graft morphology and function after recellularization of decellularized rat livers. *J Tissue Eng Regen Med*. Dec 13.

Chani B, Puri V, Sobti RC, Jha V, Puri S. 2017. Decellularized scaffold of cryopreserved rat kidney retains its recellularization potential. *PLoS One*. Mar 7;12(3):e0173040.

Choi SH, Chun SY, Chae SY, Kim JR, Oh SH, *et al*. 2015. Development of a porcine renal extracellular matrix scaffold as a platform for kidney regeneration. *J Biomed Mater Res A*. Apr;103(4):1391-403.

Costa A, Naranjo JD, Londono R, Badylak SF. 2017. Biologic Scaffolds. Cold Spring Harb Perspect Med. Mar 20. pii: a025676.

D'Alimonte I, Mastrangelo F, Giuliani P, Pierdomenico L, Marchisio M, *et al*. 2017. Osteogenic Differentiation of Mesenchymal Stromal Cells: A Comparative Analysis Between Human Subcutaneous Adipose Tissue and Dental Pulp. Stem Cells Dev. Mar 13.

Gonçalves LF, Fernandes AP, Cosme-Silva L, Colombo FA, Martins NS, *et al*. 2016. Effect of EDTA on TGF-β1 released from the dentin matrix and its influence on dental pulp stem cell migration. *Braz Oral Res*. Dec 22; 30(1):e131.

Grobstein C. 1956. Inductive tissue interaction in development. *Adv Cancer Res*.; 4:187-236.

Grobstein C. 1956. Trans-filter induction of tubules in mouse metanephrogenic mesenchyme. *Exp Cell Res*. Apr; 10(2):424-40.

Guyette JP, Charest JM, Mills RW, Jank BJ, Moser PT, *et al*. (2016. Bioengineering Human Myocardium on Native Extracellular Matrix. Circ Res. Jan 8;118(1):56-72.

Hassanein W, Uluer MC, Langford J, Woodall JD, Cimeno A *et al*. 2017. Recellularization via the bile duct supports functional allogenic and xenogenic cell growth on a decellularized rat liver scaffold. Organogenesis. Jan 2;13(1):16-27.

Holmes D. 2014. Stem cells: Decorin has role in differentiation. Nat Rev Nephrol. Feb;10(2):65.

Huang Z1, Godkin O, Schulze-Tanzil G. 2017. The Challenge in Using Mesenchymal Stromal Cells for Recellularization of Decellularized Cartilage. *Stem Cell Rev*. Feb;13(1):50-67.

Huleihel L, Hussey GS, Naranjo JD, Zhang L, Dziki JL, *et al*. 2016. Matrix-bound nanovesicles within ECM bioscaffolds. *Sci Adv*. Jun 10;2(6):e1600502.

Huynh NC, Everts V, Nifuji A, Pavasant P, Ampornaramveth RS. 2017. Histone deacetylase inhibition enhances in-vivo

bone regeneration induced by human periodontal ligament cells. Bone. Feb;95:76-84.

Inker LA, Coresh J, Sang Y, Hsu CY, Foster MC, *et al*. 2017. Filtration Markers as Predictors of ESRD and Mortality: Individual Participant Data Meta-Analysis. *Clin J Am Soc Nephrol.* Jan 6;12(1):69-78.

Kim LG, Caplin B, Cleary F, Hull SA, Griffith K, *et al*. 2017. Accounting for overdispersion when determining primary care outliers for the identification of chronic kidney disease: learning from the National Chronic Kidney Disease Audit. Nephrol Dial Transplant. Jan 17.

Kuevda EV, Gubareva EA, Gumenyuk IS, Sotnichenko AS, Gilevich IV *et al*. 2017. Modification of Rat Lung Decellularization Protocol Based on Dynamic Conductometry of Working Solution. *Bull Exp Biol Med.* Mar 31.

Li PK, Chow KM, Van de Luijtgaarden MW, Johnson DW, Jager KJ *et al*. 2017. Changes in the worldwide epidemiology of peritoneal dialysis. Nat Rev Nephrol. Feb;13(2):90-103.

Liu WY, Lin SG, Zhuo RY, Xie YY, Pan W, *et al*. 2017. Xenogeneic Decellularized Scaffold: A Novel Platform for Ovary Regeneration. *Tissue Eng Part C Methods*. Feb; 23(2):61-71.

Liu ZZ, Wong ML, Griffiths LG. 2016. Effect of bovine pericardial extracellular matrix scaffold niche on seeded human mesenchymal stem cell function. *Sci Rep.* Nov 15;6:37089.

Ma C, Wei Q, Cao B, Cheng X, Tian J, *et al*. 2017. A multifunctional bioactive material that stimulates osteogenesis and promotes the vascularization bone marrow stem cells and their resistance to bacterial infection. *PLoS One.* Mar 30;12(3):e0172499.

Matsuo I, Kimura-Yoshida C. 2014. Extracellular distribution of diffusible growth factors controlled by heparan sulfate proteoglycans during mammalian embryogenesis. Philos *Trans R Soc Lond B Biol Sci.* Dec 5;369(1657).

Mende M, Bednarek C, Wawryszyn M, Sauter P, Biskup MB, *et al*. 2016. Chemical Synthesis of Glycosaminoglycans. *Chem Rev*. Jul 27;116(14):8193-255.

Momtahan N, Panahi T, Poornejad N, Stewart MG, Vance BR, *et al*. 2016. Using Hemolysis as a Novel Method for Assessment of Cytotoxicity and Blood Compatibility of Decellularized Heart Tissues. ASAIO J. May-Jun;62(3):340-8.

Napierala H, Hillebrandt KH, Haep N, Tang P, Tintemann M, *et al*. 2017. Engineering an endocrine Neo-Pancreas by repopulation of a decellularized rat pancreas with islets of Langerhans. Sci Rep. Feb 2;7:41777.

Nigam SK1, Bush KT. 2014. Growth factor-heparan sulfate "switches" regulating stages of branching morphogenesis. Pediatr Nephrol. Apr;29(4):727-35.

O'Neill JD, Anfang R, Anandappa A, Costa J, Javidfar J, *et al*. 2013. Decellularization of human and porcine lung tissues for pulmonary tissue engineering. Ann Thorac Surg. Sep;96(3):1046-55.

Oryan A, Alidadi S, Bigham-Sadegh A, Moshiri A, Kamali A. 2017. Effectiveness of tissue engineered chitosan-gelatin composite scaffold loaded with human platelet gel in regeneration of critical sized radial bone defect in rat. J Control Release. Mar 28. pii: S0168-3659(16)31095-1.

Ott HC. 2015. Perfusion Decellularization of Discarded Human Kidneys: A Valuable Platform for Organ Regeneration. Transplantation. Sep;99(9):1753.

Peloso A, Petrosyan A, Da Sacco S, Booth C, Zambon JP, *et al*. 2015. Renal Extracellular Matrix Scaffolds From Discarded Kidneys Maintain Glomerular Morphometry and Vascular Resilience and Retains Critical Growth Factors. Transplantation. Sep;99(9):1807-16.

Pietsch J, Gass S, Nebuloni S, Echegoyen D, Riwaldt S, *et al*. 2017. Three-dimensional growth of human endothelial cells in an automated cell culture experiment container during the SpaceX CRS-8 ISS space mission - The SPHEROIDS project. Biomaterials. Apr;124:126-156.

Poornejad N, Schaumann LB, Buckmiller EM, Momtahan N, Gassman JR, *et al*. 2016. The impact of decellularization agents on renal tissue extracellular matrix. J Biomater Appl. Oct;31(4):521-533.

Przekora A, Ginalska G. 2017. Chitosan/β-1,3-glucan/hydroxyapatite bone scaffold enhances osteogenic differentiation through TNF-α-mediated mechanism. Mater Sci Eng C Mater Biol Appl. Apr 1;73:225-233.

Pu L, Wu J, Pan X, Hou Z, Zhang J, *et al*. 2017. Determining the optimal protocol for preparing an acellular scaffold of tissue engineered small-diameter blood vessels. J Biomed Mater Res B Appl Biomater. Mar 8.

Qiao WH, Liu P, Hu D, Al Shirbini M, Zhou XM, *et al*. 2016. Sequential hydrophile and lipophile solubilization as an efficient method for decellularization of porcine aortic valve leaflets: structure, mechanical property and biocompatibility study. J Tissue Eng Regen Med. Dec 13.

Quack I, Westenfeld R. 2016. Cardiovascular morbidity and mortality in patients with kidney disease. Dtsch Med Wochenschr. Nov;141(24):1771-1776.

Remuzzi A, Figliuzzi M, Bonandrini B, Silvani S, Azzollini N, *et al*. 2017. Experimental Evaluation of Kidney Regeneration by Organ Scaffold Recellularization. Sci Rep. Mar 7;7:43502.

Roth SP, Glauche SM, Plenge A, Erbe I, Heller S, *et al*. 2017. Automated freeze-thaw cycles for decellularization of tendon tissue - a pilot study. BMC Biotechnol. Feb 14;17(1):13.

Sambi M, Chow T, Whiteley J, Li M, Chua S, *et al*. 2017. Acellular Mouse Kidney ECM can be Used as a Three-Dimensional Substrate to Test the Differentiation Potential of Embryonic Stem Cell Derived Renal Progenitors. Stem Cell Rev. Feb 27.

Santoro R, Consolo F, Spiccia M, Piola M, Kassem S, *et al*. 2016. Feasibility of pig and human-derived aortic valve interstitial cells seeding on fixative-free decellularized animal pericardium. J Biomed Mater Res B Appl Biomater. Feb;104(2):345-56.

Sariola H, Peault B, LeDouarin N, Buck C, Dieterlen-Lièvre F, *et al*. 1984. Extracellular matrix and capillary ingrowth in interspecies chimeric kidneys. Cell Differ. Nov;15(1):43-51.

Sariola H, Timpl R, von der Mark K, Mayne R, Fitch JM, *et al*. 1984. Dual origin of glomerular basement membrane. Dev Biol. Jan;101(1):86-96.

Seyler TM, Bracey DN, Plate JF, Lively MO, Mannava S, *et al*. 2017. The Development of a Xenograft-Derived Scaffold for Tendon and Ligament Reconstruction Using a Decellularization and Oxidation Protocol. Arthroscopy. Feb;33(2):374-386.

Song XF, Tian H, Zhang ZX. 2016. Differential activation of CD95-mediated apoptosis related proteins in proximal and distal tubules during rat renal development. *Tissue Cell.* Oct;48(5):417-24.

Song Y. 2016. Function of Membrane-Associated Proteoglycans in the Regulation of Satellite Cell Growth. *Adv Exp Med Biol.* 900:61-95.

Sumida K, Molnar MZ, Potukuchi PK, Thomas F, Lu JL, *et al.* 2017. Blood Pressure Before Initiation of Maintenance Dialysis and Subsequent Mortality. *Am J Kidney Dis. Ma*r 10. pii: S0272-6386(17)30506-1.

Taal MW. 2016. Chronic kidney disease: towards a risk-based approach. Clin Med (Lond). Dec;16(Suppl 6): s117-s120.

Tang XS, Shen Q, Chen J, Zha XL, Xu H. 2016. Maternal protein restriction reduces perlecan at mid-metanephrogenesis in rats. Nephrology (Carlton). Mar;21(3):200-8.

Taylor DA, Parikh RB, Sampaio LC. 2017. Bioengineering Hearts: Simple yet Complex. *Curr Stem Cell Rep.;*3(1):35-44.

Thuret R, Kleinclauss F, Terrier N, Karam G, Timsit MO. 2016. Challenges in renal transplantation. *Prog Urol.* Nov; 26(15):1001-1044.

Wang L, Zhou PC, Zhu SS, Wang Y, Fan XJ, *et al.* 2017. Three-dimensional circulation perfusion culture of hepatocytes in the liver decellularizedscaffold. Zhonghua Yi Xue Za Zhi. Jan 24;97(4):265-269.

Webster AC, Nagler EV, Morton RL, Masson P. 2017. Chronic Kidney Disease. Lancet. Mar 25;389(10075):1238-1252.

Wong ML, Wong JL, Vapniarsky N, Griffiths LG. 2016. In vivo xenogeneic scaffold fate is determined by residual antigenicity and extracellular matrix preservation. Biomaterials. Jun;92:1-12.

Xu K, Kuntz LA, Foehr P, Kuempel K, Wagner A, Tuebel J, Deimling CV, Burgkart RH. 2017. Efficient decellularization for tissue engineering of the tendon-bone interface with preservation of biomechanics. PLoS One. Feb 7;12(2):e0171577.

Yoganarasimha S, Trahan WR, Best AM, Bowlin GL, Kitten TO, *et al.* 2014. Peracetic acid: a practical agent for sterilizing heat-labile polymeric tissue-engineering scaffolds. Tissue Eng Part C Methods. Sep;20(9):714-23.

Yoong RK, Mooppil N, Khoo EY, Newman SP, Lee VY, *et al.* 2017. Prevalence and determinants of anxiety and depression in end stage renal disease (ESRD). A comparison between ESRD patients with and without coexisting diabetes mellitus. J Psychosom Res. Mar;94:68-72.

Zhang L, Qiao M, Gao H, Hu B, Tan H, *et al.* 2016. Investigation of mechanism of bone regeneration in a porous biodegradable calcium phosphate (CaP) scaffold by a combination of a multi-scale agent-based model and experimental optimization/validation. Nanoscale. Aug 21;8(31):14877-87

Zhou H, Kitano K, Ren X, Rajab TK, Wu M, *et al.* 2017. Bioengineering Human Lung Grafts on Porcine Matrix. Ann Surg. Jan 12.

Zhou Z, Chaudhari P, Yang H, Fang AP, Zhao J, *et al.* 2017. Healthcare Resource Use, Costs, and Disease Progression Associated with Diabetic Nephropathy in Adults with Type 2 Diabetes: A Retrospective Observational Study. Diabetes Ther. Mar 30.

****